

Superposition MIMO Coding for the Broadcast of Layered Sources

Seok-Ho Chang, *Member, IEEE*, Minjoong Rim, *Member, IEEE*, Pamela C. Cosman, *Fellow, IEEE*,
and Laurence B. Milstein, *Fellow, IEEE*

Abstract—We propose superposition multiple-input multiple-output (MIMO) coding for the transmission of unequally important sources in a point-to-multipoint system. First, a tradeoff between Alamouti code and spatial multiplexing (V-BLAST) is analyzed in terms of the average bit error rate (BER), where the maximum data rates of both MIMO schemes are set to be equal. The results show that for a given target bit error rate, Alamouti code is preferable for a low data rate, and spatial multiplexing is preferable for a high data rate. For layered sources such as scalable video, the more important component typically has lower data rate than does the less important component. Based on these, we construct a superposition MIMO scheme where two different MIMO techniques are hierarchically combined such that important data is Alamouti coded, less important data is spatially multiplexed, and then two unequally important data symbols are superposed.

Index Terms—Alamouti code, cross-layer design, hierarchical modulation, multimedia communications, multiple-input multiple-output (MIMO) systems, spatial multiplexing, superposition, wireless video.

I. INTRODUCTION

PROGRESSIVE image and scalable video encoders [1]–[3] employ a mode of transmission such that, as more bits are received, the source can be reconstructed with better quality. These progressive sources have steadily decreasing importance for bits later in the stream, and hence unequal error protection (UEP) is a natural way to ensure their reliable transmission over mobile radio channels.

Theoretical investigation of efficient communication from a single source to multiple receivers established that optimal broadcast transmission could be achieved by a superposition transmission scheme [4]–[6]. Since the theoretical basis for UEP was initiated by [4], much of the work has shown that one practical method of achieving UEP is based on a constellation of nonuniformly spaced signal points [7]–[9], which is called a hierarchical constellation. In this constellation, more important bits in a symbol have larger minimum Euclidian distance than less important bits. As a simple example, Fig. 1 shows a

hierarchical 16 QAM constellation [10]. The 16 signal points are divided into four clusters, and each cluster consists of four signal points. Bits i_1 and q_1 have minimum Euclidian distance d_M , and bits i_2 and q_2 have minimum Euclidian distance d_L . The distance ratio $\alpha = d_M/d_L (> 1.0)$ determines how much more i_1 and q_1 are protected against errors than are i_2 and q_2 . A hierarchical 16 QAM constellation, denoted by 4/16 QAM, can be viewed as a superposition of two QPSK subconstellations. For low SNR, it operates as only a basic QPSK subconstellation having larger minimum distance. For high SNR, hierarchical 16 QAM can operate as both basic and secondary QPSK subconstellations. Hierarchical modulation has been intensively studied for digital broadcasting systems [7]–[9], and the Digital Video Broadcasting (DVB-T) standard [10], which is now commercially available, incorporated hierarchical QAM for layered video data transmission.

Multiple-input multiple-output (MIMO) systems have received a great deal of attention. Two popular approaches for MIMO systems are spatial diversity and multiplexing. Transmit diversity [11]–[13] is an approach where information is spread across multiple transmit antennas to maximize spatial diversity. Spatial multiplexing [14]–[16] is an approach whereby independent information is transmitted on each antenna, and thus data rate is increased.

We propose superposition MIMO coding for the transmission of layered sources, such as progressive images or scalable video, in a point-to-multipoint system. In a transmission such as broadcasting or multicasting, a single source transmits an encoded signal to multiple receivers. Each receiver experiences different channel conditions depending on its location. Even if channel state information for each receiver were available at the transmitter, the modulation alphabet size and the MIMO mode cannot be adapted due to the nature of broadcasting. We first analyze the tradeoff between the transmit diversity and spatial multiplexing schemes under the constraint that the two schemes have the same maximum data rate. We consider Alamouti coding [11] and V-BLAST [14] as the transmit diversity and spatial multiplexing schemes, respectively. In this analysis, the modulation alphabet sizes for both MIMO schemes are chosen to be different, such that the maximum data rates are the same. The results show that for a given target bit error rate (BER), an Alamouti code is preferable to spatial multiplexing for a low data rate (i.e., small alphabet size), and vice versa for a high data rate (i.e., large alphabet size). This is presented in Section II.

In layered sources, important components and less important components do not have the same data rate in general. A typical example is scalable video. The base layer, which is more important, has a smaller number of bits than does

Paper approved by I. Lee, the Editor for Wireless Communication Theory of the IEEE Communications Society. Manuscript received March 5, 2010; revised December 19, 2010 and April 16, 2011.

S.-H. Chang was with the Department of Electrical and Computer Engineering, University of California at San Diego, La Jolla, CA, 92093-0407, USA. He is now with Qualcomm Inc., San Diego, CA, 92121-1714, USA (e-mail: seokhoc@qualcomm.com).

P. C. Cosman and L. B. Milstein are with the Department of Electrical and Computer Engineering, University of California at San Diego, La Jolla, CA, 92093-0407, USA (e-mail: pcosman@ucsd.edu; milstein@ece.ucsd.edu).

M. Rim is with the Department of Information and Communication Engineering, Dongguk University, Seoul, Korea (e-mail: minjoong@dongguk.edu).

This research was supported by the US Army Research Office under MURI, grant number W911NF-04-1-0224, and by the National Science Foundation under grant number CCF-0915727.

Digital Object Identifier 10.1109/TCOMM.2011.090911.100112

the enhancement layer. Therefore, when a layered source is broadcast hierarchically in MIMO systems, a tradeoff between transmit diversity and spatial multiplexing schemes should be considered for each layer. Based on the above, in Section III, we propose a layered source broadcasting system where two different MIMO techniques are hierarchically combined. An Alamouti code is applied for the more important component, which has lower data rate, in order to maximize the performance for the receivers with poor channel qualities. Spatial multiplexing is applied for the less important component, having higher data rate, which is decoded only by receivers having good channel conditions. Superposition of two different MIMO approaches is embodied in a way that basic subconstellation symbols are encoded with an Alamouti code, secondary subconstellation streams are spatially multiplexed, and then the two subconstellations are superposed to construct the final transmit symbols. Performance evaluations are provided in Section IV, and we conclude our work in Section V.

II. COMPARISON OF ALAMOUTI CODING AND SPATIAL MULTIPLEXING HAVING THE SAME MAXIMUM DATA RATE

When the same modulation alphabet size is employed for both spatial multiplexing and transmit diversity schemes, the former achieves better peak-signal-to-noise ratio (PSNR)¹ performance at high SNR due to a increased data rate, whereas the latter retains robustness at low SNR. Since we are considering a broadcast transmission where a single source transmits data to multiple receivers having various channel qualities, we cannot optimally switch between two different MIMO modes (i.e., both modulation and MIMO mode are fixed). For this case, as a way to compare both MIMO schemes fairly, the maximum data rates of both are set to be equal.

A. Channel Model

The MIMO system is equipped with N_t transmit and N_r ($\geq N_t$) receive antennas. The propagation channel is characterized by an $N_r \times N_t$ matrix \mathbf{H} whose element h_{jk} at the j th row and k th column is the channel gain from the k th transmit antenna to the j th receive antenna, and the h_{jk} 's are assumed to be i.i.d complex Gaussian random variables with zero mean and unit variance. The received signal $\mathbf{y} = [y_1 \cdots y_{N_r}]^T$ can be expressed as $\mathbf{y} = \mathbf{H}\mathbf{s} + \mathbf{n}$, where $\mathbf{s} = [s_1 \cdots s_{N_t}]^T$ is the transmit symbol, and $\mathbf{n} = [n_1 \cdots n_{N_r}]^T$ is the noise whose elements are assumed to be i.i.d. complex Gaussian random variables with zero mean and variance of σ_n^2 .

B. Average BER

The average BER of an M -ary square QAM constellation for SISO systems in an AWGN channel is given by [17, eq. (14)]. Let γ_s denote the signal-to-noise ratio (SNR) per symbol. We define $\gamma_s \triangleq E[|s_k|^2]/\sigma_n^2$ ($k = 1, \dots, N_t$), where s_k is the k th component of the transmit symbol vector \mathbf{s} . For the Alamouti scheme, the instantaneous post-processing SNR per symbol is a chi-square random variable with $2N_tN_r$ degrees of freedom [18]. The same constellation symbol, s_k ,

is transmitted twice during two symbol time periods [11], and thus for an M -ary QAM, the SNR per bit, γ_b , is given by $\gamma_b = 2 \times \gamma_s / \log_2 M$. From the above discussion, it can be shown that the exact BER of the Alamouti scheme for an M -ary square QAM constellation is given by²

$$P_{b,Alamouti} = \frac{4}{\sqrt{M} \log_2 M} \sum_{k=1}^{\log_2 \sqrt{M}} \sum_{i=0}^{(1-2^{-k})\sqrt{M}-1} \left[(-1)^{\lfloor \frac{i \cdot 2^{k-1}}{\sqrt{M}} \rfloor} \left(2^{k-1} - \left\lfloor \frac{i \cdot 2^{k-1}}{\sqrt{M}} + \frac{1}{2} \right\rfloor \right) \left(\frac{1-\mu(i)}{2} \right)^{N_t N_r} \right. \\ \left. \times \sum_{j=0}^{N_t N_r - 1} \left\{ \binom{N_t N_r - 1 + j}{j} \left(\frac{1+\mu(i)}{2} \right)^j \right\} \right] \quad (1)$$

where

$$\mu(i) = \sqrt{\frac{3(2i+1)^2 (\log_2 M) \gamma_b}{4(M-1) + 3(2i+1)^2 (\log_2 M) \gamma_b}}.$$

We next derive the average BER for spatial multiplexing. It has been shown that for a zero forcing (ZF) receiver, the instantaneous post-processing SNR on each independent transmit stream is a chi-square random variable with $2(N_r - N_t + 1)$ degrees of freedom [19][20], and thus the exact BER expression is achievable. For spatial multiplexing, the SNR per bit is given by $\gamma_b = \gamma_s / \log_2 M$. It can be shown that the exact BER of the spatial multiplexing with a ZF receiver for an M -ary square QAM constellation is given by

$$P_{b,SM-ZF} = \frac{4}{\sqrt{M} \log_2 M} \sum_{k=1}^{\log_2 \sqrt{M}} \sum_{i=0}^{(1-2^{-k})\sqrt{M}-1} \left[(-1)^{\lfloor \frac{i \cdot 2^{k-1}}{\sqrt{M}} \rfloor} \right. \\ \left. \times \left(2^{k-1} - \left\lfloor \frac{i \cdot 2^{k-1}}{\sqrt{M}} + \frac{1}{2} \right\rfloor \right) \left(\frac{1-\mu(i)}{2} \right)^{N_r - N_t + 1} \right. \\ \left. \times \sum_{j=0}^{N_r - N_t} \left\{ \binom{N_r - N_t + j}{j} \left(\frac{1+\mu(i)}{2} \right)^j \right\} \right] \quad (2)$$

where

$$\mu(i) = \sqrt{\frac{3(2i+1)^2 (\log_2 M) \gamma_b}{2(M-1) + 3(2i+1)^2 (\log_2 M) \gamma_b}}.$$

C. High SNR Approximation (Minimum Euclidian Distance Approximation) of the Average BER

For high SNR, the BER is approximated by the error function term having the minimum Euclidian distance. If we discard the terms having non-minimum Euclidian distances, we have

$$P_{b,Alamouti} \approx \frac{4(\sqrt{M}-1)}{\sqrt{M} \log_2 M} \left(\frac{1-\mu}{2} \right)^{N_t N_r} \\ \times \sum_{j=0}^{N_t N_r - 1} \binom{N_t N_r - 1 + j}{j} \left(\frac{1+\mu}{2} \right)^j \quad (3)$$

where $\mu = \sqrt{3(\log_2 M)\gamma_b / \{4(M-1) + 3(\log_2 M)\gamma_b\}}$. Further, for high SNR, μ can be approximated as $\mu \approx 1 -$

¹ PSNR is a common performance index of images or video, and is inversely proportional to the mean square error of the source.

² The detailed steps of all the analysis in Section II can be found in [21].

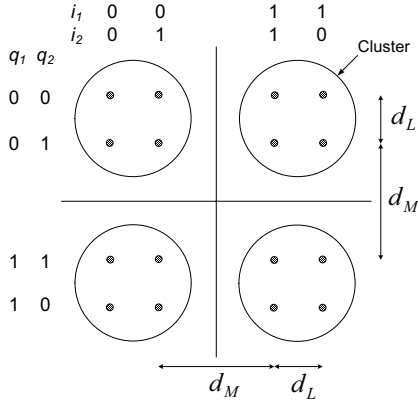


Fig. 1. Hierarchical 16 QAM constellation.

$\frac{2(M-1)}{3(\log_2 M)\gamma_b}$, where we have used $\sqrt{\frac{x}{1+x}} \approx 1 - \frac{1}{2x}$ for $x \gg 1$. From this, it can be shown that (3) can be rewritten as

$$P_{b,Alamouti} \approx P_{b,Alamouti}^{app} = \left(\frac{2N_t N_r - 1}{N_t N_r} \right) \frac{4(\sqrt{M} - 1)}{\sqrt{M} \log_2 M} \left(\frac{M-1}{3 \log_2 M} \right)^{N_t N_r} \left(\frac{1}{\gamma_b} \right)^{N_t N_r} \quad (4)$$

In the same way, it can be shown that, for high SNR, $P_{b,SM-ZF}$ can be approximated as

$$P_{b,SM-ZF} \approx P_{b,SM-ZF}^{app} = \binom{2(N_r - N_t) + 1}{N_r - N_t + 1} \times \frac{4(\sqrt{M} - 1)}{\sqrt{M} \log_2 M} \left(\frac{M-1}{6 \log_2 M} \right)^{N_r - N_t + 1} \left(\frac{1}{\gamma_b} \right)^{N_r - N_t + 1} \quad (5)$$

D. Comparison of High SNR BERs of Alamouti Scheme and Spatial Multiplexing for the Same Maximum Data Rate

1) *Crossover point for SNR*: We compare the high SNR approximate BERs of the Alamouti scheme and the spatial multiplexing scheme having the same maximum data rate. To do this, we employ m -ary QAM for spatial multiplexing, and m^2 -ary QAM for the Alamouti scheme. It is assumed that m is greater than or equal to 4 (i.e., QPSK). Note that $N_r \geq N_t = 2$. If we let $M = m^2$ in (4), we have

$$P_{b,Alamouti}^{app} = \left(\frac{4N_r - 1}{2N_r} \right) \frac{2(m-1)}{m \log_2 m} \left(\frac{m^2 - 1}{6 \log_2 m} \right)^{2N_r} \left(\frac{1}{\gamma_b} \right)^{2N_r} \quad (6)$$

If we let $M = m$ in (5), we have

$$P_{b,SM-ZF}^{app} = \binom{2N_r - 3}{N_r - 1} \frac{4(\sqrt{m} - 1)}{\sqrt{m} \log_2 m} \left(\frac{m-1}{6 \log_2 m} \right)^{N_r - 1} \left(\frac{1}{\gamma_b} \right)^{N_r - 1} \quad (7)$$

We now find the SNR, γ_b^* , for which (6) and (7) are the same. That is,

$$\begin{aligned} & \left(\frac{4N_r - 1}{2N_r} \right) \frac{2(m-1)}{m \log_2 m} \left(\frac{m^2 - 1}{6 \log_2 m} \right)^{2N_r} \left(\frac{1}{\gamma_b^*} \right)^{2N_r} \\ &= \binom{2N_r - 3}{N_r - 1} \frac{4(\sqrt{m} - 1)}{\sqrt{m} \log_2 m} \left(\frac{m-1}{6 \log_2 m} \right)^{N_r - 1} \left(\frac{1}{\gamma_b^*} \right)^{N_r - 1} \end{aligned} \quad (8)$$

It can be shown that the γ_b^* satisfying (8) is given by

$$\gamma_b^* = \left\{ \frac{\binom{4N_r - 1}{2N_r} \sqrt{m} + 1}{2 \binom{2N_r - 3}{N_r - 1} 6^{N_r + 1} \sqrt{m}} \times \frac{(m-1)^{N_r + 1} (m+1)^{2N_r}}{(\log_2 m)^{N_r + 1}} \right\}^{\frac{1}{N_r + 1}} \quad (9)$$

Further, it can be shown that for $m \geq 4$, γ_b^* is a strictly increasing function in m . That is, as the alphabet size, m , increases, γ_b^* strictly increases, regardless of the number of receive antennas.

2) *Crossover point for BER*: It can be shown that if we substitute γ_b^* , given by (9), into (6), the corresponding BER, P_b^* , is given by

$$P_b^* = 2 \binom{4N_r - 1}{2N_r} \left\{ \frac{2 \binom{2N_r - 3}{N_r - 1}}{\binom{4N_r - 1}{2N_r}} \right\}^{\frac{2N_r}{N_r + 1}} \times \frac{m-1}{m \log_2 m} \left(\frac{\sqrt{m}}{\sqrt{m} + 1} \right)^{\frac{2N_r}{N_r + 1}} \left(\frac{1}{m+1} \right)^{\frac{2N_r(N_r - 1)}{N_r + 1}} \quad (10)$$

Let

$$g(m) = \frac{m-1}{m \log_2 m} \left(\frac{1}{\sqrt{m} + 1} \right)^{\frac{2N_r}{N_r + 1}} \times \left(\frac{\sqrt{m}}{m+1} \right)^{\frac{2N_r}{N_r + 1}} \left(\frac{1}{m+1} \right)^{\frac{2N_r(N_r - 2)}{N_r + 1}} \quad (11)$$

We let $g_1(m) = \sqrt{m}/(m+1)$, and $g_2(m) = (m-1)/(m \log_2 m)$. Then, for $m \geq 4$, we have $dg_1(m)/dm < 0$. We also have

$$\frac{dg_2(m)}{dm} = \frac{\log_2 m - \frac{m}{\ln 2} + \frac{1}{\ln 2}}{(m \log_2 m)^2} < 0 \quad (12)$$

where the inequality is derived from the following:

- i) Let $h(m)$ be the numerator of $dg_2(m)/dm$.
- ii) For $m \geq 4$, we have $dh(m)/dm = (1-m)/(m \ln 2) < 0$. Further, $h(4) = 2 - 3/\ln 2 < 0$.
- iii) Hence, $h(m) < 0$ for $m \geq 4$

From (11) and (12), $g(m)$ is a strictly decreasing function in m . From (10) and (11), as the alphabet size, m , increases, P_b^* strictly decreases, regardless of the number of receive antennas.

3) *Comparison of the BERs*: From (6) and (7), it can be shown that the ratio of $P_{b,Alamouti}^{app}$ to $P_{b,SM-ZF}^{app}$, denoted by $R(\gamma_b)$, is a strictly decreasing function in γ_b . Thus, from $R(\gamma_b^*) = 1$, we have

$$\begin{aligned} P_{b,Alamouti}^{app} &< P_{b,SM-ZF}^{app} \quad \text{for } \gamma_b > \gamma_b^* \\ P_{b,Alamouti}^{app} &> P_{b,SM-ZF}^{app} \quad \text{for } \gamma_b < \gamma_b^* \end{aligned} \quad (13)$$

Let $P_{b,1}^*$ and $\gamma_{b,1}^*$ denote the crossover point when a modulation alphabet size $m = C_1$ is employed, and $P_{b,2}^*$ and $\gamma_{b,2}^*$ denote the crossover point when an alphabet size $m = C_2$ is used. Suppose that $C_1 < C_2$. Then, from the results below (9) and (12), we have

$$\gamma_{b,1}^* < \gamma_{b,2}^* \quad \text{and} \quad P_{b,1}^* > P_{b,2}^*. \quad (14)$$

Based on (13) and (14), the high SNR BERs of the Alamouti scheme and spatial multiplexing with ZF receiver for the

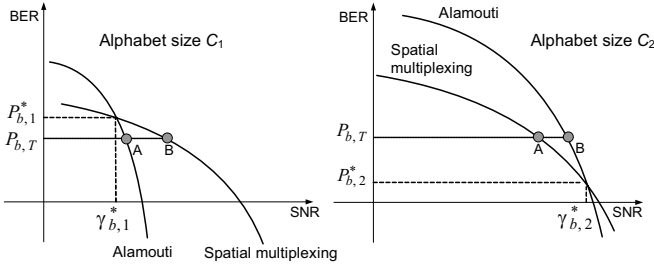


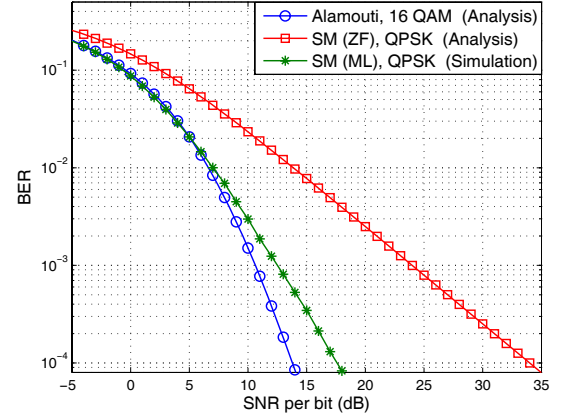
Fig. 2. High SNR approximate BERs of the Alamouti and spatial multiplexing schemes for the same maximum data rate. For alphabet size $C_1 < C_2$, these BERs have the following properties: i) $\gamma_{b,1}^* < \gamma_{b,2}^*$ ii) $P_{b,1}^* > P_{b,2}^*$ iii) $P_{b,i,Alamouti}^{app} < P_{b,i,SM-ZF}^{app}$ for $\gamma_{b,i} > \gamma_{b,i}^*$, and $P_{b,i,Alamouti}^{app} > P_{b,i,SM-ZF}^{app}$ for $\gamma_{b,i} < \gamma_{b,i}^*$ ($i = 1, 2$).

same maximum data rate are qualitatively depicted in Fig. 2. Suppose that a target bit error rate, $P_{b,T}$, is smaller than $P_{b,1}^*$ but greater than $P_{b,2}^*$. Then, from Fig. 2, the Alamouti scheme is preferable for an alphabet size C_1 , whereas spatial multiplexing is preferable for an alphabet size C_2 . From here onwards, for a given $P_{b,T}$, we refer to an alphabet size which satisfies $P_b^* > P_{b,T}$ as a small alphabet size (i.e., low data rate), and refer to an alphabet size which satisfies $P_b^* < P_{b,T}$ as a large alphabet size (i.e., high data rate).

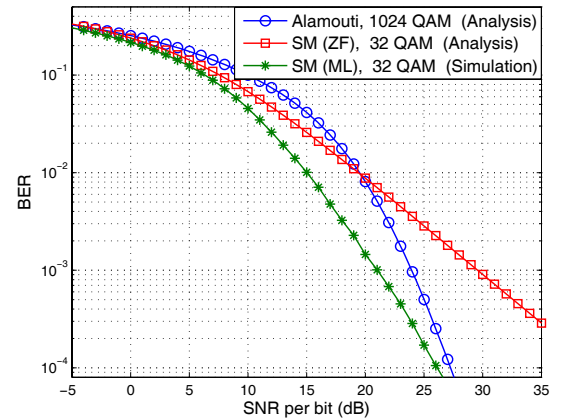
Using (1) and (2), we evaluate the exact BERs for 2×2 MIMO systems for various maximum data rates (i.e., alphabet sizes). The results are shown in Fig. 3 (more results can be found in [21]). The BER performance of spatial multiplexing with the optimal maximum likelihood (ML) receiver is also plotted. We note that since the exact BER of the ML receiver is not analyzable, the curve is obtained from the simulation. It is observed that as the alphabet size increases, the crossover point for the BERs of the Alamouti scheme and spatial multiplexing with ZF receiver, γ_b^* and P_b^* , moves in a way predicted by the analysis based on the high SNR BER expressions (see Fig. 2). Further, as the alphabet size increases, the crossover point for the Alamouti and the spatial multiplexing with an ML receiver moves in the same way as that for the Alamouti and spatial multiplexing with a ZF receiver. If we focus on a BER of 10^{-4} , the Alamouti scheme outperforms spatial multiplexing with the ML receiver for the data rate of 4 bits per symbol period (Fig. 3 (a)), whereas the latter outperforms the former for the data rate of 10 bits per symbol period (Fig. 3 (b)). The two schemes perform roughly the same for the data rate of 8 bits per symbol period (this can be found in [21]). We again note that this preference depends on the target bit error rate of an application. For example, if the $P_{b,T}$ is 10^{-6} , the Alamouti scheme is preferable, even for the data rate of 10 bits per symbol period.

III. SUPERPOSITION OF ALAMOUTI CODE AND SPATIAL MULTIPLEXING

For layered sources, more important components and less important components do not necessarily have the same data rate. From this, we are motivated to apply different MIMO approaches for each component of layered sources for a hierarchical broadcast. In particular, we consider the case where the more important component has lower data rate



(a) The maximum data rate: 4 bits per symbol period (Alamouti code for 16 QAM and spatial multiplexing for QPSK).



(b) The maximum data rate: 10 bits per symbol period (Alamouti code for 1024 QAM and spatial multiplexing for 32 QAM).

Fig. 3. The exact BERs of the Alamouti scheme and spatial multiplexing for various alphabet sizes (i.e., for various maximum data rates) in 2×2 MIMO systems (SM denotes spatial multiplexing).

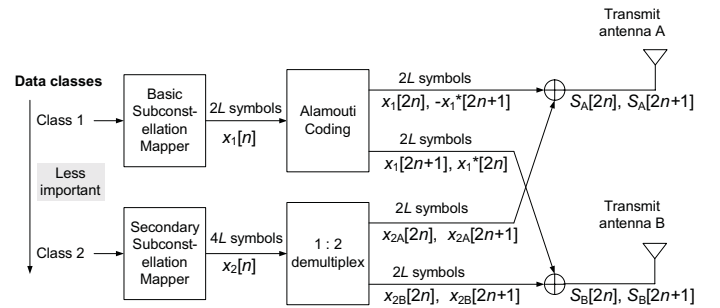


Fig. 4. Superposition MIMO coding: two different MIMO codes are hierarchically combined such that Alamouti coding is applied for the low-rate more important data, and spatial multiplexing is applied for the high-rate less important data.

than does the less important component (a typical example is scalable video).

The proposed superposition MIMO scheme is depicted in Fig. 4. We denote the basic subconstellation symbols by $x_1[n]$ ($n = 0, 1, \dots, 2L - 1$), and the secondary subconstellation symbols by $x_2[n]$ ($n = 0, 1, \dots, 4L - 1$). We demultiplex

$x_2[n]$ into two transmit antenna streams such that $x_{2A}[n] = x_2[2n]$ and $x_{2B}[n] = x_2[2n + 1]$ ($n = 0, 1, \dots, 2L - 1$). Then, for $n = 0, 1, \dots, L - 1$, the final transmit symbols of the proposed scheme are given by

$$\begin{bmatrix} S_A[2n] & S_A[2n + 1] \\ S_B[2n] & S_B[2n + 1] \end{bmatrix} = \begin{bmatrix} x_1[2n] + x_{2A}[2n] & -x_1^*[2n + 1] + x_{2A}[2n + 1] \\ x_1[2n + 1] + x_{2B}[2n] & x_1^*[2n] + x_{2B}[2n + 1] \end{bmatrix} \quad (15)$$

where each row corresponds to a transmit antenna and each column corresponds to a time symbol. In the following, we present the decoding of the proposed scheme. Note that, since Alamouti code is applied to the basic subconstellation in the proposed scheme (see eq. (15)), ML decoding has to be performed during two symbol time periods for both the basic and the secondary subconstellations (i.e., for an entire hierarchical constellation). Since this requires a complex receiver, we consider successive decoding as follows:

- 1) Alamouti decoding is performed for the basic subconstellation.
- 2) The decoded basic subconstellation is subtracted from the received signal.
- 3) Spatial demultiplexing (such as ML, MMSE (minimum mean square error), or ZF decoding) is performed for the secondary subconstellation.

Note that in step 3, spatial demultiplexing such as ML decoding can be performed during one symbol time period, since the basic subconstellation encoded with an Alamouti code has already been subtracted in step 2. This implies that even if ML decoding is used in step 3, the complexity of successive decoding is much less than that of the optimal ML decoding of an entire hierarchical constellation. From (15), it is seen that when the basic subconstellation symbols, $x_1[2n]$ and $x_1[2n + 1]$, are Alamouti decoded in step 1, the secondary subconstellation symbols, $x_{2A}[2n]$, $x_{2A}[2n + 1]$, $x_{2B}[2n]$, and $x_{2B}[2n + 1]$, act as interference. Therefore, the performance of the successive decoding depends on the distance ratio, α , of the hierarchical constellation, since the distance ratio is related to the energy difference between the basic and secondary subconstellations (note that the distance ratio is defined as the ratio of the minimum Euclidian distance of the basic subconstellation to that of the secondary subconstellation). The BER performance of the optimal ML decoding and successive decoding are compared in 2×2 MIMO systems for hierarchical 4/16 QAM with distance ratios of 2.0 and 4.0 (these are typical ratios for a hierarchical QAM constellation [10]). In successive decoding, ML decoding is performed in step 3. The results are shown in Fig. 5. For a distance ratio of $\alpha = 2.0$, the performance of successive decoding is slightly worse than that of the optimal ML decoding. For a distance ratio of $\alpha = 4.0$, both decoders perform roughly the same.

IV. PERFORMANCE EVALUATION

We evaluate the PSNR performance of the proposed superposition code. In this evaluation, we consider hierarchical 4/64 QAM which consists of a QPSK basic subconstellation and a 16 QAM secondary subconstellation. Note that for one symbol time period and two transmit antennas, the proposed

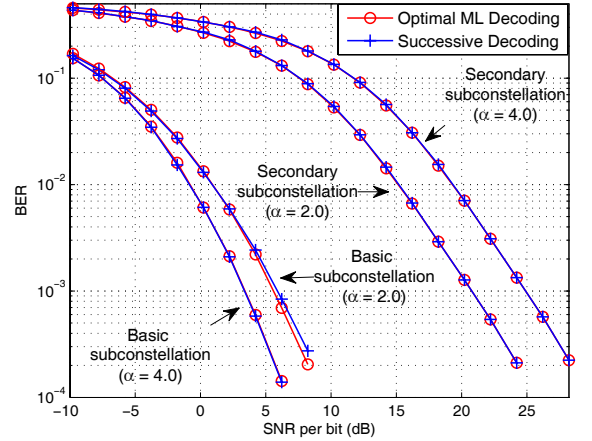


Fig. 5. The BER performance of the optimal ML decoding and successive decoding of the proposed scheme in 2×2 MIMO systems. For successive decoding, ML decoding is performed for spatial demultiplexing of the secondary subconstellation.

scheme transmits 2 bits for the more important component (2 bits (QPSK) with an Alamouti code), and 8 bits for the less important component (4 bits (16 QAM) \times 2 (spatial multiplexing)). For comparison purposes, we also evaluate the performance of the transmission schemes where different MIMO approaches are not superposed. The first scheme is hierarchical 2/32 QAM with spatial multiplexing, and the second scheme is hierarchical 4/1024 QAM with an Alamouti code.³ We refer to these as pure spatial multiplexing and pure Alamouti schemes. Note that the above three schemes have the same maximum data rate, both for the more important and the less important components. We use the optimal ML decoding for the pure spatial multiplexing and the pure Alamouti scheme. For the proposed scheme, we use successive decoding, where the secondary subconstellation is decoded with ML decoding. In our evaluation, error correction coding is not considered.

We evaluate the performance for 2×2 MIMO systems using the source coder SPIHT [1] as an example, and provide the results for the standard 8 bits per pixel (bpp) 512 \times 512 Lena image with a transmission rate of 0.375 bpp. We assume that the transmitted signal experiences a slow fading channel such that channel coefficients are nearly constant over an image, and that channel estimation at the receiver is perfect. The end-to-end performance is measured by the expected distortion of the image or video frame. In the following, we describe the evaluation of the expected distortion, $E[D]$, in detail. The system takes the compressed progressive bitstream from the source encoder, and transforms it into a sequence of packets. Then, as shown in Fig. 4, the packets are encoded by the space-time codes. At the receiver, if a received packet is correctly decoded, the next packet is considered by the source decoder. Otherwise, the decoding is stopped and the source is reconstructed from only the correctly decoded packets due to

³ Hierarchical 2/32 QAM consists of a BPSK basic subconstellation and a 16 QAM secondary subconstellation. Hierarchical 4/1024 QAM consists of a QPSK basic subconstellation and a 256 QAM secondary subconstellation.

the nature of multimedia progressive source code. We assume that all decoding errors in a packet can be detected by the use of a cyclic redundancy check (CRC).

Let $P_i(\eta_i)$ denote the probability of a decoding error of packet i ($1 \leq i \leq N$), where η_i is the SNR per symbol and N is the number of transmitted packets. Then, the probability that no decoding errors occur in the first n packets, but an error does occur in the next one, $P_{c,n}$, is given by

$$P_{c,n} = P_{n+1}(\eta_{n+1}) \prod_{i=1}^n (1 - P_i(\eta_i)) \quad (16)$$

for $1 \leq n \leq N-1$. Note that $P_{c,0} = P_1(\eta_1)$ is the probability of an error in the first packet, and $P_{c,N} = \prod_{i=1}^N (1 - P_i(\eta_i))$ is the probability that all N packets are correctly decoded. Let d_n denote the distortion of the source using the first n packets for the source decoder ($0 \leq n \leq N$). The d_n can be expressed as $d_n = D(\sum_{i=1}^n r_i)$, where r_i is the number of source bits in packet i , $D(x)$ denotes the operational rate-distortion function of the source, and $d_0 = D(0)$ refers to the distortion when the decoder reconstructs the source without any of the received information. Then, the expected distortion of the source, $E[D]$, can be expressed as

$$\begin{aligned} E[D] &= \sum_{n=0}^N d_n P_{c,n} \\ &= D(0)P_{c,0} + \sum_{n=1}^N D\left(\sum_{i=1}^n r_i\right) P_{c,n}. \end{aligned} \quad (17)$$

For the uncoded system considered in this paper, the probability of a decoding error of packet i , $P_i(\eta_i)$, can be expressed as

$$P_i(\eta_i) = 1 - \{1 - P_{b,i}(\eta_i)\}^{r_i} \quad (18)$$

where $P_{b,i}(\eta_i)$ is the BER for packet i . Note that $P_{b,i}(\eta_i)$ depends on the modulation parameters, such as alphabet size and distance ratio of the hierarchical constellation employed for packet i . As stated before, it is assumed that the transmitted signal experiences slow Rayleigh fading, in which channel coefficients are nearly constant over an image frame. With this channel model, from (16)–(18), the expected distortion for the uncoded system can be expressed as

$$\begin{aligned} E[D] &= \int_0^\infty \int_0^\infty \cdots \int_0^\infty \left\{ D(0) \left(1 - \{1 - P_{b,1}(\eta_1)\}^{r_1}\right) \right. \\ &+ \sum_{n=1}^{N-1} D\left(\sum_{i=1}^n r_i\right) \left[\left(1 - \{1 - P_{b,n+1}(\eta_{n+1})\}^{r_{n+1}}\right) \right. \\ &\left. \left. \prod_{i=1}^n \{1 - P_{b,i}(\eta_i)\}^{r_i}\right] + D\left(\sum_{i=1}^N r_i\right) \prod_{i=1}^N \{1 - P_{b,i}(\eta_i)\}^{r_i} \right\} \\ &f(\eta_1) f(\eta_2) \cdots f(\eta_N) d\eta_1 d\eta_2 \cdots d\eta_N \end{aligned} \quad (19)$$

where $f(\eta_i)$ is the probability density function (PDF) of η_i , the instantaneous post-processing SNR per symbol at the receiver. Note that $f(\eta_i)$ depends on the space-time code applied to packet i , as well as its decoding algorithm at the receiver. Note also that the expression in (19) includes powers of $P_{b,i}(\eta_i)$ in its integral. Thus, the evaluation of (19) requires the computation for the expectation of the powers of $Q(x)$ (i.e., $E[Q^n(x)]$) with respect to the random post-processing

SNR that characterizes the space-time code and its decoding algorithm at the receiver. Further, the PDF, $f(\eta_i)$, is known only for some limited cases, such as the Alamouti scheme and the zero-forcing receiver for spatial multiplexing. For these reasons, we calculate $E[D]$ by simulation. Note that $D(0)$ in (19) indicates the distortion for the event that there is an error in the first packet with probability $P_{c,0}$, which is given below (16). For a still image, $D(0)$ means reconstructing the entire image at the mean pixel value, so the image is worthless. For a video, on the other hand, the decoder will hold over the previous frame for that frame. For low motion videos, $D(0)$ might not be large. Note that $E[D]$ is a function of the channel SNR and the distance ratio of the hierarchical constellation. For a performance comparison, for each MIMO scheme, we find the optimal distance ratio of a hierarchical constellation which minimizes the expected distortion over a range of average SNRs using the weighted cost function

$$\arg \min_{\alpha} \frac{\int_0^\infty \omega(\gamma_b) E[D] d\gamma_b}{\int_0^\infty \omega(\gamma_b) d\gamma_b} \quad (20)$$

where α is a distance ratio, and $w(\gamma_b)$ in $[0, 1]$ is the weight function. For example, $w(\gamma_b)$ is given by

$$\omega(\gamma_b) = \begin{cases} 1, & \text{for } \gamma_b^A \leq \gamma_b \leq \gamma_b^B \\ 0, & \text{otherwise.} \end{cases} \quad (21)$$

Note that in broadcast systems, the weight function in (21) indicates that average SNRs of multiple receivers are uniformly distributed in the range of $\gamma_b^A \leq \gamma_b \leq \gamma_b^B$. Eq. (20) indicates that α is chosen such that the sum of the expected distortion of the receivers distributed in the range of $\gamma_b^A \leq \gamma_b \leq \gamma_b^B$ is minimized. To compare the image quality, we use PSNR defined as

$$\text{PSNR} = 10 \log \frac{255^2}{E[D]} \quad (\text{dB}) \quad (22)$$

where $E[D]$ is given by (19). We present the PSNR performance of each MIMO scheme by evaluating (19)–(22) as follows: We first compute (20) using both the expected distortion $E[D]$, given by (19), which is calculated by simulation, and the weight function, $w(\gamma_b)$, given by (21). Next, with the distance ratio of α obtained in (20), we evaluate the PSNR using (19) and (22) over a range of average SNRs given by (21).

The PSNR performance of the proposed superposition code is compared with those of the two pure MIMO schemes in Fig. 6 (more results can be found in [21]). For reference, the performance of the optimal ML decoding of the proposed scheme is also plotted. On the average, the proposed scheme has a channel SNR gain of about 2dB, and a PSNR gain of about 1dB, compared to the other MIMO schemes. This is because the Alamouti scheme outperforms spatial multiplexing for the basic subconstellation supporting a low data rate, and spatial multiplexing outperforms the Alamouti scheme for the secondary subconstellation supporting a high data rate, as indicated in Section II.

Lastly, in the following, we compare the performances of the proposed superposition code and the Golden code [22]. Note that linear dispersion codes and algebraic codes [23][24] have been studied to pursue the benefits of both

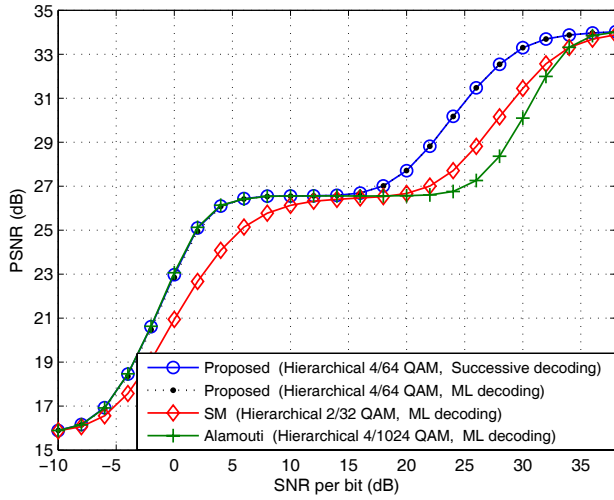


Fig. 6. The PSNR performances of the proposed superposition code, pure Alamouti scheme, and pure spatial multiplexing scheme in 2×2 MIMO systems. The SNR range of the weight function is 0–38 dB (i.e., $\gamma_b^A = 0$ dB and $\gamma_b^B = 38$ dB in (21)).

spatial diversity and multiplexing. Algebraic codes, such as the Golden code, achieve the optimal diversity-multiplexing tradeoff [25] in two-input multiple-output (TIMO) systems, though they, in general, have higher receiver complexity than either spatial multiplexing or the Alamouti code.

We evaluate the PSNR performance for the optimal ML decoding of the Golden code. Hierarchical 2/32 QAM is employed for the Golden code such that it has the same data rates for both the more important component (2 bits per symbol period) and the less important component (8 bits per symbol period) as does the proposed scheme. The result is shown in Fig. 7. It is seen that the performance of the proposed scheme is slightly better than or equal to that of the Golden code for SNRs up to about 27 dB, whereas the Golden code slightly outperforms the proposed scheme for SNRs greater than about 27 dB. Note that for each MIMO scheme, using (20), the distance ratio of the hierarchical constellation is optimized to minimize the expected distortion over a range of average SNRs. Unlike the cases for either pure spatial multiplexing or the pure Alamouti scheme shown in Fig. 6, from Fig. 7, we cannot clearly see a preference between the proposed scheme and the Golden code in terms of their PSNR performances. Thus, for comparison purposes, we consider slightly increasing the distance ratio of the hierarchical constellation employed by the Golden code scheme; Doing so, more energy is allotted to the basic subconstellation, which is decoded by the low SNR receivers, and less energy is assigned to the secondary subconstellation, decoded only by high SNR receivers. As a result, the PSNR performance for low SNR receivers would improve, while the PSNR for high SNR receivers would degrade. Specifically, we increase the distance ratio for the Golden code scheme such that it provides the same performance as the proposed scheme for low SNR receivers. The resultant PSNR curve is also shown in Fig. 7 (see the dashed curve with cross marks). It is observed that

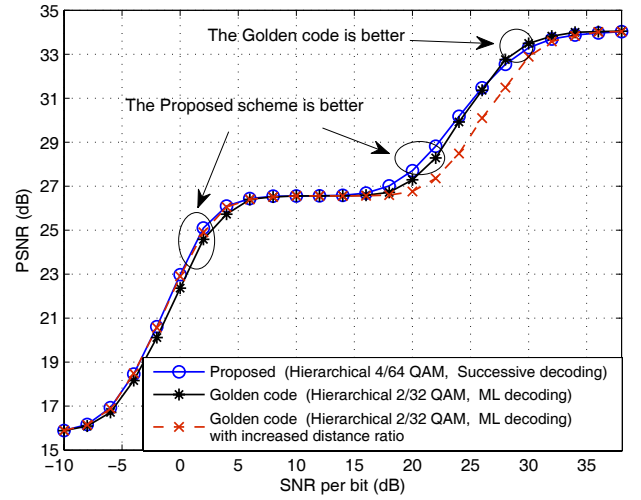


Fig. 7. The PSNR performances of the proposed superposition code and the Golden code in 2×2 MIMO systems. The SNR range of the weight function is 0–38 dB (i.e., $\gamma_b^A = 0$ dB and $\gamma_b^B = 38$ dB in (21)).

the Golden code with the increased distance ratio performs the same as the proposed scheme for low SNRs (less than about 16 dB), but the latter outperforms the former for high SNRs (greater than about 16 dB). Thus, the proposed scheme slightly outperforms the Golden code, and this will be discussed below.

The BER performances of the Golden code, the Alamouti scheme and spatial multiplexing are evaluated in the same way as we did in Section II. We first compare the Golden code with the Alamouti scheme for various data rates, as is shown in Fig. 8 (a). It is seen that for a high data rate, such as 8 bits per symbol period, the performance of the Alamouti scheme is much worse than that of the Golden code. However, as the data rate decreases, the performance gap between the Golden code and the Alamouti scheme decreases; for a data rate of 4 bits per symbol period, the performance of the Alamouti scheme is slightly worse than that of the Golden code. Further, the Alamouti scheme outperforms the Golden code for a data rate of 2 bits per symbol period. Note that for multimedia layered sources such as scalable video, the base layer, which is more important than the enhancement layer, consists of a smaller number of bits, but requires very low error rate. In other words, the base layer is the low-rate important component demanding low target error rate. Also note that the proposed superposition code employs the Alamouti scheme to encode the base layer. Hence, from Fig. 8 (a), it is expected that the decoding performance of the base layer for the proposed scheme would be roughly comparable to that for the Golden code scheme.

We next compare the Golden code with spatial multiplexing for various data rates. From Fig. 8 (b), it is seen that for a low data rate, such as 4 bits-per-symbol period, the performance of the spatial multiplexing is much worse than that of the Golden code. However, it is observed that as the data rate increases, the performance gap between the two schemes decreases. For a high data rate, such as 8 or 10 bits-per-symbol period, the performance of spatial multiplexing is

roughly the same as that of the Golden code at a high bit error rate. More precisely, both schemes would have nearly identical performance if the target error rate is greater than about 10^{-2} (note that this is the uncoded BER). Recall that the proposed superposition code employs the spatial multiplexing to encode the enhancement layer, which is high-rate, but is the less important component. Hence, from Fig. 8 (b), it is expected that the decoding performance of the enhancement layer for the proposed scheme would be comparable to that of the Golden code scheme.

From the above, it is expected that regarding the broadcast of multimedia layered sources, the proposed scheme, which superposes two simple component codes (the Alamouti and spatial multiplexing), would have performance roughly comparable to that of the Golden code. This is because, for the proposed superposition code, the two component codes work well in different regimes where each has a strong advantage in terms of data rates and target error rates.

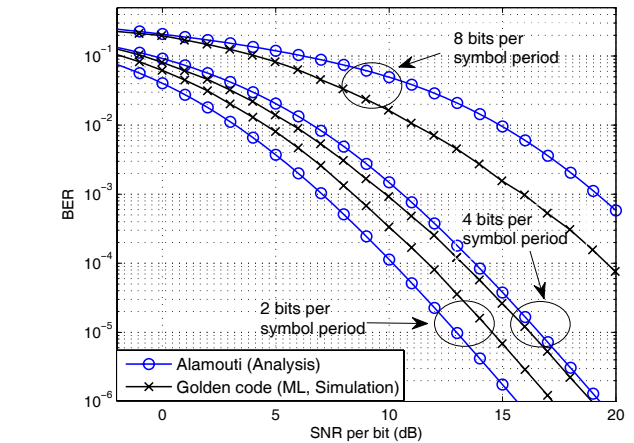
Along with the performance, we note that the significantly unequal decoding complexity between the Golden code and the orthogonal space time codes (i.e., the Alamouti code) for the base layer also should be considered for the design of a system. Recently, it was shown that the Golden code can be optimally ML decoded with complexity proportional to $M^{2.5}$ for an M -ary QAM constellation [26]. Note that the complexity of the ML decoding of spatial multiplexing is proportional to M^2 . Hence, if the Golden code is to be used, the additional decoding complexity of $\mathcal{O}(M^{2.5})/\mathcal{O}(M^2) = \mathcal{O}(\sqrt{M})$ for the enhancement layer should be considered, especially when the constellation size for the high data-rate enhancement layer, M , is large.

V. CONCLUSION

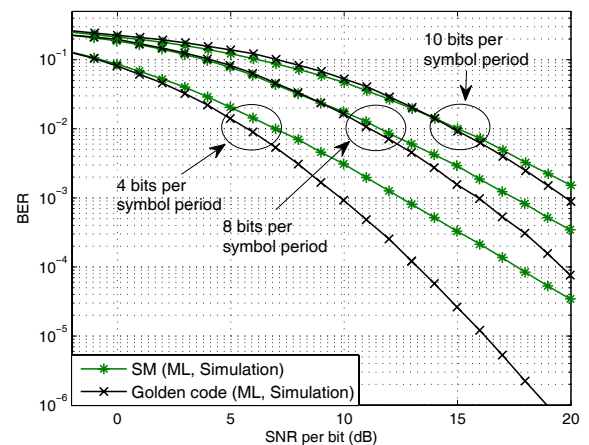
We proposed superposition MIMO coding for the broadcast of unequally important sources. The tradeoff between an Alamouti code and spatial multiplexing having the same maximum data rate was analyzed. The results showed that for a given target bit error rate, the Alamouti code is preferable for a low data rate, and spatial multiplexing is preferable for a high data rate. Based on this, in the proposed scheme, two different MIMO techniques are hierarchically combined such that the low-rate important component is Alamouti encoded, the high-rate less important component is spatially multiplexed, and then the two differently encoded symbols are superposed. A successive decoding algorithm was presented. Due to the sufficiently large energy difference between the subconstellations in the hierarchical broadcast of a layered source, this decoding was shown to have performance nearly identical to that of the complex optimal ML decoding. Performance evaluation showed that the PSNR of the proposed superposition code is much better than that of the pure spatial multiplexing scheme or the pure Alamouti scheme, and is roughly comparable to that of the complex Golden code scheme, in the broadcast of multimedia layered sources.

REFERENCES

[1] A. Said and W. A. Pearlman, "A new, fast, and efficient image codec based on set partitioning in hierarchical trees," *IEEE Trans. Circuits Syst. Video Technol.*, vol. 6, no. 3, pp. 243–249, June 1996.



(a) Comparison of the Golden code with the Alamouti scheme



(b) Comparison of the Golden code with spatial multiplexing

Fig. 8. The exact BER performances of the Golden code (ML decoding), the Alamouti scheme, and spatial multiplexing (ML decoding) for various maximum data rates in 2×2 MIMO systems.

[2] D. Taubman and M. Marcellin, *JPEG2000: Image Compression Fundamentals, Standards, and Practice*. Kluwer, 2001.

[3] H. Schwarz, D. Marpe, and T. Wiegand, "Overview of the scalable video coding extension of H.264/AVC," *IEEE Trans. Circuits Syst. Video Technol.*, vol. 17, no. 9, pp. 1103–1120, Sep. 2007.

[4] T. Cover, "Broadcast channels," *IEEE Trans. Inf. Theory*, vol. 18, no. 1, pp. 2–14, Jan. 1972.

[5] P. P. Bergmans, "Random coding theorem for broadcast channels with degraded components," *IEEE Trans. Inf. Theory*, vol. 19, no. 2, pp. 197–207, Mar. 1973.

[6] E. C. van der Meulen, "A survey of multi-way channels in information theory: 1961–1976," *IEEE Trans. Inf. Theory*, vol. 23, no. 1, pp. 1–37, Jan. 1977.

[7] K. Ramchandran, A. Ortega, K. M. Uz, and M. Vetterli, "Multiresolution broadcast for digital HDTV using joint source/channel coding," *IEEE J. Sel. Areas Commun.*, vol. 11, no. 1, pp. 6–23, Jan. 1993.

[8] A. R. Calderbank and N. Seshadri, "Multilevel codes for unequal error protection," *IEEE Trans. Inf. Theory*, vol. 39, no. 4, pp. 1234–1248, July 1993.

[9] M. Morimoto, H. Harada, M. Okada, and S. Komaki, "A study on power assignment of hierarchical modulation schemes for digital broadcasting," *IEICE Trans. Commun.*, vol. E77-B, pp. 1495–1500, Dec. 1994.

[10] "Digital Video Broadcasting (DVB); Framing Structure, Channel Coding and Modulation for Digital Terrestrial Television," ETSI EN 300 744 V1.5.1, Nov. 2004.

[11] S. M. Alamouti, "A simple transmit diversity technique for wireless

- communications," *IEEE J. Sel. Areas Commun.*, vol. 16, no. 8, pp. 1451–1458, Oct. 1998.
- [12] V. Tarokh, N. Seshadri, and A. R. Calderbank, "Space-time codes for high data rate wireless communication: performance criterion and code construction," *IEEE Trans. Inf. Theory*, vol. 44, no. 2, pp. 744–765, Mar. 1998.
- [13] V. Tarokh, H. Jafarkhani, and A. R. Calderbank, "Space-time block codes from orthogonal designs," *IEEE Trans. Inf. Theory*, vol. 45, no. 5, pp. 1456–1467, July 1999.
- [14] G. J. Foschini, "Layered space-time architecture for wireless communication in a fading environment when using multiple antennas," *Bell Labs. Tech. J.*, vol. 1, no. 2, pp. 41–59, 1996.
- [15] P. W. Wolniansky, G. J. Foschini, G. D. Golden, and R. A. Valenzuela, "V-BLAST: an architecture for realizing very high data rates over the rich-scattering wireless channel," in *Proc. URSI Int. Symp. Signals, Syst., Electron.*, Sep. 1998, pp. 295–300.
- [16] G. J. Foschini and M. J. Gans, "On limits of wireless communications in a fading environment when using multiple antennas," *Wireless Pers. Commun.*, vol. 6, no. 3, pp. 311–335, Mar. 1998.
- [17] K. Cho and D. Yoon, "On the general BER expression of one- and two-dimensional amplitude modulations," *IEEE Trans. Commun.*, vol. 50, no. 7, pp. 1074–1080, July 2002.
- [18] A. Paulraj, R. Nabar, and D. Gore, *Introduction to Space-Time Wireless Communications*. Cambridge University Press, 2003.
- [19] J. Winters, J. Salz, and R. D. Gitlin, "The impact of antenna diversity on the capacity of wireless communication systems," *IEEE Trans. Commun.*, vol. 42, no. 234, pp. 1740–1751, Feb./Mar./Apr. 1994.
- [20] D. Gore, R. W. Heath Jr., and A. Paulraj, "On performance of the zero forcing receiver in presence of transmit correlation," in *Proc. Int. Symp. Inf. Theory*, 2002, p. 159.
- [21] S.-H. Chang, "Joint optimization of physical and application layers for wireless multimedia communications," Ph.D. dissertation, University of California, San Diego, 2010.
- [22] J.-C. Belfiore, G. Rekaya, and E. Viterbo, "The Golden code: a 2×2 full-rate space-time code with non-vanishing determinants," *IEEE Trans. Inf. Theory*, vol. 51, no. 4, pp. 1432–1436, Apr. 2005.
- [23] R. W. Heath Jr. and A. Paulraj, "Linear dispersion codes for MIMO systems based on frame theory," *IEEE Trans. Signal Process.*, vol. 50, no. 10, pp. 2429–2441, Oct. 2002.
- [24] P. Dayal and M. K. Varanasi, "An optimal two transmit antenna space-time code and its stacked extensions," *IEEE Trans. Inf. Theory*, vol. 51, no. 12, pp. 4348–4355, Dec. 2005.
- [25] L. Zheng and D. N. C. Tse, "Diversity and multiplexing: a fundamental tradeoff in multiple-antenna channels," *IEEE Trans. Inf. Theory*, vol. 49, no. 5, pp. 1073–1096, May 2003.
- [26] M. O. Sinnokrot and J. R. Barry, "Fast maximum-likelihood decoding of the Golden code," *IEEE Trans. Wireless Commun.*, vol. 9, no. 1, pp. 26–31, Jan. 2010.